UNIVERSIDAD DISTRITAL
FRANCISCO JOSÉ DE CALDAS

Visión Electrónica
https://doi.org/10.14483/issn.2248-4728

VISIÓN ELECTRÓNICA

A RESEARCH VISION

Thermal, mechanical and magnetostatic analysis for 1u cubesat systems: finite volume simulation

Análisis térmico, mecánico y magnetoestático para sistemas cubesat 1u: simulación con volúmenes finitos

Paula Andrea Duran Parra[1], Emanuel Quiroga Neisa[2], Maria Paula Valero Bohórquez [3], Héctor Guillermo Parra Peñuela[3], Diego Alfonso Rojas Sarmiento[3]

INFORMACIÓN DEL ARTÍCULO

Historia del artículo:
Enviado: 04/08/2025
Recibido: 25/09/2025
Aceptado: 17/11/2025

Keywords:
Heat transfer
CubeSat 1U
Network Communication
Radiation
Finite Volumes

Palabras clave:
Transferencia de calor
CubeSat 1U
Redes de comunicaciones
Radiación
Volúmenes finitos

ABSTRACT

The CubeSat 1U will be developed using ANSYS simulations, allowing a comparison between the most common materials in artificial satellites (titanium, copper and aluminum) in terms of metric, magnetic and thermal performance. Firstly, the metric analysis will involve the realization of a model of the stresses and deformations during the launch stage, which will generate maximum loads of 4.55 g under the controlled conditions of an Ariane 5 type rocket. The magnetic analysis will be related to the simulation of the fields generated to maintain the CubeSat orientation based on the magnetization of a structural wall. The thermal analysis involves the modeling of heat flow methods by conduction, convection and radiation and involves the study of the structure in terms of temperature variation and its performance under them. The objective of the above analyses is to achieve an optimal result for the performance characteristics of CubeSat in terms of strength, Hindu control and thermal transfer to obtain the best possible performance in the atmosphere.

RESUMEN

El CubeSat 1U se desarrollará utilizando simulaciones en ANSYS, permitiendo una comparación entre los materiales más comunes en satélites artificiales (titanio, cobre y aluminio) en cuanto a su desempeño métrico, magnético y térmico. En primer lugar, el análisis métrico involucrará la realización de un modelo de los esfuerzos y deformaciones durante la etapa del lanzamiento, el cual generará

1. Bachelor's degree in Mechatronics Engineering, Nueva Granada Military University, Colombia. Student: Universidad Militar Nueva Granada, Colombia. Military University, Colombia. Email: est.paulaa.duran@unimilitar.edu.co ORCID: https://orcid.org/0009-0008-5410-9657
2. Bachelor's degree in Mechatronics Engineering, Nueva Granada Military University, Colombia. Student: Universidad Militar Nueva Granada, Colombia. Email: est.emanuel.quiroga@unimilitar.edu.co ORCID: https://orcid.org/0009-0009-3557-3726
3. Bachelor's degree in Mechatronics Engineering, Nueva Granada Military University, Colombia. Student: Universidad Militar Nueva Granada, Colombia. Email: est.mariap.valero@unimilitar.edu.co ORCID: https://orcid.org/0009-0008-1108-6598
4. Electronic Engineer, Universidad Distrital Francisco José de Caldas, Colombia. PhD in Engineering, Universidad Distrital Francisco José de Caldas, Colombia. Full-time Professor: Universidad Militar Nueva Granada - Mechatronics Engineering Program, Colombia, .hector.parra@unimilitar.edu.co Email:ORCID: https://orcid.org/0000-0002-6184-8000
5. Mechtronics Engineer, Universidad Militar Nueva Granada, Colombia. Magister en Ingeniería Mecatrónica, Universidad Militar Nueva Granada. Full-Time Professor: Universidad Militar Nueva Granada - Mechatronics Engineering Program, Colombia. E-mail: diego.rojass@unimilitar.edu.co ORCID: https://orcid.org/0000-0002-2962-6061

Cite this article as: P. A. Duran-Parra, E. Quiroga-Neisa, M. P. Valero-Bohórquez, H. G. Parra-Peñuela, D. A. Rojas-Sarmiento, "Thermal, mechanical and magnetostatic analysis for 1u cubesat systems: finite volume simulation", Visión Electrónica, vol. 19, no. 2, 2025.

cargas máximas de 4.55 g bajo las condiciones controladas de un cohete de tipo Ariane 5. El análisis magnético se relacionará con la simulación de los campos generados para mantener la orientación de CubeSat sobra la base de la magnetización de una pared estructural. El análisis térmico involucra el modelamiento de los métodos de flujo de calores por conducción, convección y radiación e involucra el estudio de la estructura en términos de la variación de temperatura y su desempeño bajo ellas. El objetivo de los análisis anteriores es lograr un resultado óptimo para las características de desempeño de CubeSat en términos de resistencia, control de hindú y transferencia térmica con el fin de obtener el mejor desempeño posible en la atmósfera.

1. Introduction

The proposal is based on the need to optimize the design of a 1U CubeSat capable of withstanding the extreme conditions of launch and space operation, maximizing efficiency in terms of mechanical strength, orientation control and thermal management. Currently, the design of these satellites faces limitations in terms of materials that allow an adequate balance between strength, weight, magnetic capacity for orientation control and thermal behavior in space. The proposal seeks to evaluate different materials (titanium, copper and aluminum) and configurations through simulations that represent real operating conditions, in order to select the combination that best meets these requirements and contributes to improve the overall performance of the CubeSat.

1.1. State of the art

1.1.1. Thermal analysis

Regarding heat transfer and thermal analysis in the design and simulation of CubeSats, the phenomenon has already been extensively discussed through the laws of thermodynamics, which explain the thermal behavior of systems and allow predicting their conditions under a variety of environmental factors. Among these conditions, the temperature in capacity to measure thermal energy is critical to determine the internal conditions of CubeSat and its response in various situations. One aspect of the laws of thermodynamics is Fourier's Law which describes the process of heat transfer through the solid when there is a temperature difference, which promotes the flow from the hotter area to the colder area. For convection policy, another relevant aspect of heat transfer involves heat transfers between a solid and a fluid. It can be natural or forced and was applied by Newton's cooling law, determining the relationship between the rate of temperature difference and the difference between an object and its environment cooling terms. Finally, radiation was aquatic to describe heat transfer through the vacuum discontinuity in the form of electromagnetic waves, as it is a particularly important process in the phenomenon where CubeSats operate [1].

Fourier's law

Fourier's law: characterized by conduction flow which indicates that the rate of heat transferred through a solid material is proportional to its cross-sectional area and conductivity coefficient and the temperature gradient, but inversely proportional to the length of the conduction path[1]. Eventually, the law led to the establishment of the basis in the design and analysis of temperature problems.

$$\dot{q} = -K \cdot \nabla T \tag{1}$$

$$q_x = -K \cdot \frac{dT}{dx} \tag{2}$$

Where q_X is considered to be the conduction heat flux density in the X direction (W/m^2), K is the thermal conductivity of the material, $W/m.k$; and dT/dx is the temperature gradient with respect to the position.

Newton's cooling law

Newton's law of cooling stipulates that the rate of temperature change of an object is directly proportional to the temperature difference between the object and its surroundings. In convection, the law explains how a body gives up heat to the fluid[2].

$$\dot{q} = hA(T_s - T_f) \tag{3}$$

It can be expressed mathematically as h as the heat flux, where is the convective heat transfer coefficient, A is the surface area, A is the surface temperature and A is the fluid temperature. During the thermal analysis of CubeSats, several models have been developed to closely examine the behavior of these heat transfer devices. Specifically, using the direct solar radiation equations, the authors have determined the amount of energy the CubeSat parts receive while illuminated by the sun through the specific absorptivity and emissivity associated with each material. The Stefan-Boltzmann Law provides an approach to measure the amount of energy emitted by these parts superficially and thus helps define the equilibrium temperature of the system by balancing the incoming and outgoing energy. [2] To conduct the most recent

study, the behavior of three common types of aerospace materials were analyzed: aluminum, copper and titanium. Using finite element simulations, the authors have examined the thermal properties around temperature, heat flux and heat flow rate as CubeSat experienced different environments. By examining these characteristics, it was possible to derive how thermal stability changes and define the relationship between the equilibrium temperature and the amount of thermal energy being emitted or absorbed, and as a result, measure the heat flow rate. In addition, the first law of thermodynamics is to understand the conditions of thermal equilibrium between the bodies themselves. Being the focal point of how temperatures between components are determined, it allows the authors to evaluate whether the CubeSat can achieve independent thermal equilibrium.

Numerical Methods Used in CubeSat Thermal Analysis The development of numerous heat transfer simulations on CubeSats has benefited greatly from the use of numerical methods. Finite element analysis, for example, provides an effective approach to model and simulate the thermal behavior of the system under different conditions[3]. FEA has been essential for the analysis of the different types of materials used to form the CubeSat, creating a robust predictive framework for the thermal response of each structural and electronic element. Based on these simulations, how solar radiation and other heat sources affect the thermal stability of the CubeSat has been studied. The heat fluxes and equilibrium temperature fluctuate considerably depending on the absorption and emission properties of the materials, highlighting the crucial importance of choosing specific materials with the appropriate thermal properties for durability during the mission[3].

1.1.2. Magnetostatic analysis

The Magnetorquer publication by Reda Lamniji, Riley Stewart and Jiayin Ling[10] is devoted to the design of a magnetorquers system for the CubeSat, designed to improve its maneuverability in space. A new system of a separate magnetic coil mounted on the PCB is developed to overcome the limitations of a current system that can only produce limited ograms and from which it is impossible to measure any of these ograms. In addition, it is proposed to take advantage of the embedded motherboard for at least one internal czsuperskillsets system test magnetometer. The authors argued that such a decision would allow the CubeSat to perform automatic troubleshooting tests. The paper covers the products needed to assemble all the parts for the magnetorquer, with a total price of 35,905 USD for materials and 1125 USD for labor price. In addition, a project plan is presented in the form of a Gantt chart, covering the stages from parts procurement to the deadline for submission of the job. The authors made constant reference to the ethical aspect of academic production, emphasizing that the protocols for providing error recognition and correction were based on the IEEE Code of Ethical Conduct. This will also be accompanied by a data sheet of a magentorquer[11] for reference magnetic flux values in Gauss.

1.1.3. Mechanical analysis

Efforts and Deformations
The evaluation of stresses and deformations is crucial with respect to the mechanical vision for design. For the analysis, the equivalent stress is employed, a scalar term derived from the three-dimensional stress tensor. This concept simplifies the evaluation of the structure for complicated loading cases, emphasizing various load axes into a correlated value.

Equivalent Stress

Typically, equivalent stress is defined in the literature through the use of the von Mises criterion, which accurately predicts the onset of failure in ductile materials. In other words, a solid will not break as long as the distortion energy does not reach the critical level for the plastic distortion observed in the tensile test graph[6].

$$\sigma_v = \sqrt{\frac{(\sigma_{xx} - \sigma_{yy})^2 + (\sigma_{yy} - \sigma_{zz})^2 + (\sigma_{zz} - \sigma_{xx})^2 + 6(\sigma_{xy}^2 + \sigma_{yz}^2 + \sigma_{zx}^2)}{2}} \tag{4}$$

Equivalent Elastic Strain
Elastic strain is the indicator of the degree of distortion that materials experience and is directly related to equivalent stress. More specifically, strain is the ratio between the elastic stiffness, Young's modulus E, and the equivalent stress[7].
This approach has two main advantages. On one hand, engineers can predict the deformation that combined stress produces within the elastic limit of the material before failure occurs.

Safety Factor
On the other hand, it is possible to evaluate agendas regarding safety factors, which are defined as the ratio of the maximum allowable stress divided by the equivalent stress. A safety factor greater than one means that the design is safe, as the material will not experience permanent deformation.

Total Deformation
It is also key to consider the total deformation suffered by the material under the applied load. This quantity is the sum of elastic deformation and plastic deformation, which is permanent once the elastic limit is exceeded. In a structural

simulation, total deformation can be used to identify areas most likely to fail during the system's lifespan, compromising the integrity of the part [8].
The ability to simulate total deformation is crucial for design in a simulator like Ansys, as it can be easily calculated and visualized, helping to optimize the design to minimize areas of high deformation. Thanks to such simulations, engineers can easily simulate extreme conditions and optimize designs based on their behavior. Such simulations in the design phase allow for the rapid generation of iterative versions that evaluate different changes with minimal effort regarding their performance. For these reasons, it is possible to apply a similar analysis to a CubeSat design process, likely more relevant considering that weight and adequate strength are fundamental given the limited space and severe loading conditions.

1.2. Methods

1.2.1. Thermal analysis

For the analysis of heat flow in a 1U (10x10x10 cm) CubeSat, an approach based on numerical simulations and thermal radiation heat transfer equations was used. Three different materials (aluminum, copper and titanium) were studied to evaluate their respective equilibrium temperatures, heat flow and heat flux when exposed to outer space. This analysis allowed us to understand the heat dissipation characteristics of each material in an environment where the CubeSat receives direct solar radiation and emits thermal radiation into space.

Materials and Properties
The three materials selected for analysis were:

Table 1: Material properties

Materials	Absorptivity	Emissivity	Thermal conductivity
Aluminum	0.2	0.005	205 W/mK
Copper	0.3	0.005	385 W/mK
Titanium	0.3	0.5	22 W/mK

The table shows the respective properties of each material needed to perform the respective simulations. In addition, the solar constant: 1361 W/m² and the Stefan-Boltzmann constant: $5{,}67x10\,{-}^{8}\,W/m^2 - K^4$ were used.

The equations used for the simulation of thermal phenomena are based on the principles of radiative heat transfer. They include the calculation of heat flow in and heat flow out, as well as the heat transfer rate per unit area (heat flux).

Direct Solar Radiation (Heat Flow In)

The amount of thermal energy absorbed by the CubeSat is calculated using the absorptivity of the material and the solar constant. The equation is as follows:

$$Q_{in} = \alpha A \cdot 1361\,\mathrm{W/m^2} \tag{5}$$

Absorptivity α is a material property that indicates what fraction of the incident radiation is absorbed. The exposed area (A) is the surface area of the material that receives the radiation, in this case $0{,}01m^2$. The solar constant (I), which has a value of 1361 W/m^2, is the amount of solar radiation reaching the Earth per unit area perpendicular to the sun's rays in outer space[5].

Emitted Radiation (Heat Flow Out)
The energy emitted by the CubeSat follows the Stefan-Boltzmann Law, described by the equation:

$$Q_{out} = \epsilon A \sigma T^4 \tag{6}$$

Emissivity (ϵ) is the ability of a material to emit thermal radiation compared to an ideal blackbody, with values between 0 and 1. The exposed area (A) is the surface area of the material in contact with the surroundings, while the Stefan-Boltzmann constant (σ) (approximately $5{,}67\times10^{-8}\,\mathrm{W/m^2K^4}$) describes the energy emitted by a blackbody according to its temperature. The temperature (T) in Kelvin also influences the amount of thermal energy the material can emit **ref5**.

1.2.2. Magnetostatic analysis

The magneto-static analysis included three types of simulations: current density, directional magnetic flux density, directional magnetic fluid density and the total force experienced by the system. This procedure was performed three times, once for each material previously mentioned (titanium, copper and aluminum), varying the voltage in each simulation. The objective was to determine what value of voltage and current allows the structure to generate the desired magnetic field of 1.5 Gauss. The previously mentioned voltage will be applied to one side of the structure generating the current flowing out of the other side.

1.2.3. Mechanical analysis

To ensure that the structure of these nanosatellites can withstand the stresses and deformations caused by the forces experienced during launch, simulations are conducted in

ANSYS. These simulations are performed with three materials commonly used in satellites: titanium, copper, and aluminum. It is essential to analyze the deformations that the preliminary design of the CubeSat 1U might experience due to the forces applied by the launch system and the associated vibrations. These forces and vibrations are the most intense that the structure will face throughout its mission.

Through simulations in ANSYS, the deformations in different materials used in the manufacturing of CubeSats, such as aluminum 6061 or titanium alloy Ti-6Al-4V, can be evaluated. To understand the magnitude of the loads acting on the structure, a static analysis must be performed, in addition to considering the dynamic load generated by the acceleration during launch, particularly in the initial stage, where the loads reach their maximum.

The following figure illustrates how the longitudinal static acceleration of the Ariane 5 launch vehicle varies in different stages, noting that the highest peak is $4{,}55g$ and occurs in the first stage, i.e., during takeoff [9].

The structure of the nanosatellites must be capable of resisting both axial and torsional loads generated by vibrations. These loads must be evaluated in each component of the structure. Using finite element software, each of these components can be analyzed in detail. According to the proposed structure, the mass of the CubeSat is $0{,}2586\,\mathrm{kg}$, assuming it is built with aluminum 6061-T6.

It is necessary to calculate the loads induced by the acceleration from the launch vehicle, which in this case will be the Ariane 5, which has a maximum acceleration of $4{,}55g$, and a safety factor of $1{,}25$ is used [5]. To calculate the total load, Equation 8 will be used:

$$F_{TE} = F_{2SAT} + F_{MP} + F_{RI} \tag{7}$$

Where F_{TE} is the quasi-static force, i.e., one that changes little over time, total applied to the structure, F_{2SAT} is the force exerted by the mass of 2 satellites when integrated into an interface and a launch spring, F_{MP} is the force exerted by the mass of the nanosatellite structure itself when accelerated, and F_{RI} is the force exerted by the spring of the interface. [5]Each of these is calculated as follows:

$$F_{2SAT} = 2{\times}1{,}33\,\mathrm{kg}{\times}4{,}55{\times}9{,}81\,\mathrm{m/s^2}{\times}1{,}25 = 148{,}4128\,\mathrm{N} \tag{8}$$

Where m is the mass of the CubeSat, A_{LV} is the maximum longitudinal acceleration of the launch vehicle (LV), and FS is the safety factor [9].

$$F_{MP} = 0{,}2586\,\mathrm{kg} \times 4{,}55 \times 9{,}81\,\mathrm{m/s^2} = 14{,}4284\,\mathrm{N} \tag{9}$$

In this case, M is the mass of the nanosatellite structure only [9].

$$F_{RI} = K{\times}X{\times}FS = 138{,}40\,\mathrm{N/m}{\times}0{,}340\,\mathrm{m}{\times}1{,}25 = 60\,\mathrm{N} \tag{10}$$

To calculate the elastic force, K is the spring constant, X is the spring displacement, and FS is the safety factor.

$$\begin{aligned} F_{TE} &= F_{2SAT} + F_{MP} + F_{RI} \\ &= 148{,}4128\,\mathrm{N} + 14{,}4284\,\mathrm{N} + 60\,\mathrm{N} \\ &= 222{,}96\,\mathrm{N} \end{aligned} \tag{11}$$

In relation to the above, to perform the structural analysis, it is necessary to apply the force at each tip of the structure, which is directly composed of the loads F_{2SAT} and F_{RI}. To determine the load applied at each tip, F_{MP} is subtracted from F_{TE}, and the resulting value is divided by 4, yielding the following equation:[5]

$$\begin{aligned} F_{PUNTA} &= \frac{F_{TE} - F_{MP}}{4} \\ &= \frac{222{,}96\,\mathrm{N} - 14{,}4284\,\mathrm{N}}{4} \\ &= 52{,}1015\,\mathrm{N} \end{aligned} \tag{12}$$

Considering the previous calculation for the analysis, the following scheme will be used, where the inertial load corresponds to the acceleration of the launch vehicle, which is 4.55g, and when multiplied by the safety factor, it yields 55.7943 m/s^2.

1.3. Analysis of results

1.3.1. Thermal analysis

The following are the respective results of the thermal analysis of the selected materials, finding the respective comparisons with respect to the equilibrium temperature, heat flow and heat flux.

Table 2: Thermal results of materials tested

Materials	Equilibrium temperature (°C)	Heat Flow (W)	Heat Flux (W/m^2)
Aluminum	123.85	7.03	703
Copper	149.55	9.012	901.2
Titanium	73.27	1.22	122

Table 2 shows the analyzed results of the three CubeSat simulated materials. In this table, the heat flux and the heat flow output of the respective materials analyzed are shown. In addition, the equilibrium temperature that approximately

each temperature would have is displayed. The thermal simulation of the Cubesat is presented below, showing the equilibrium temperature obtained and the heat transfer that is taking place on a surface.

Figure 1: CubeSat equilibrium temperature simulation for materials of a) Aluminum, b) Copper, c) Titanium.

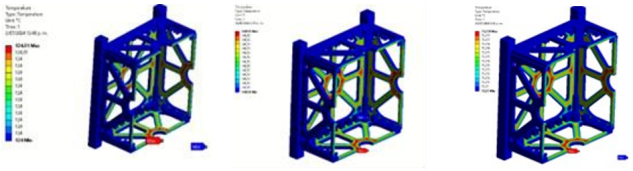

a) b) c)

Source: Own.

Figure 1 shows the simulation of the CubeSat in relation to its equilibrium temperature. This analysis was based on matching the emitted energy and absorbed energy equations to determine the equilibrium temperature. The results show that the equilibrium temperature of aluminum is approximately 123.85 °C, as seen in Figure 1.a, that of copper is 149.55 °C, as shown in Figure 1.b, and that of titanium is 73.27 °C, as seen in Figure 1.c. These values are considered the maximum temperatures in the simulation.

Figure 2: Proposed heat flux for the simulation with the material of a) Aluminum, b) Copper, c) Titanium.

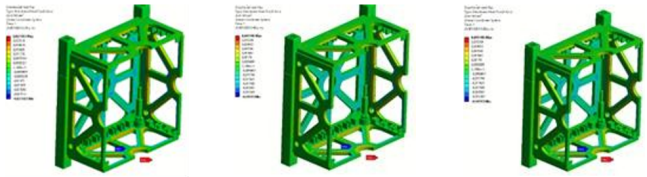

a) b) c)

Source: Own.

Figure 2 represents the total heat flux of the simulation for the CubeSat, where it is considered to be the heat transfer rate per unit area, determining that the incoming heat flux to the CubeSat for Figure 2.a is approximately 272. 2 W/m^2 and the outgoing is 703 W/m^2 for aluminum, for figure 2.b it is 408.3 W/m^2, while the outgoing flux is 901.2 W/m^2 and figure 2.c is 409.2 W/m^2, while the outgoing flux reaches 122 W/m^2 for titanium.

1.3.2. Magnetostatic analysis

The respective simulations will be carried out where the cubesat structure will be made of copper material and will be subjected to a voltage of 60 millivolts:

Figure 3: a) CubeSat current density, b) Cubesat directional magnetic flux density isometric view, c) Cubesat directional magnetic flux density range.

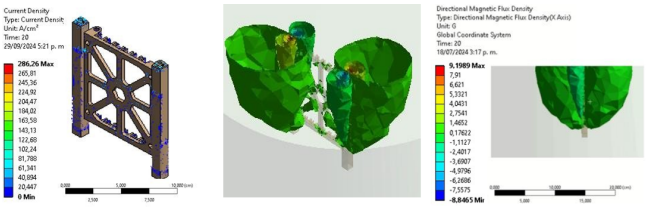

a) b) c)

Source: Own.

Figure 3.a shows the current density simulation, which allows analyzing the current passing through a cross section of the CubeSat structure. It is observed that the applied voltage generates a high current density, which could cause damage due to excessive overheating. The directional magnetic flux density simulations, presented in Figures 3.b and 3.c, reveal a magnetic flux close to 1.462 Gauss, with an approximate range of 5 cm from the structure.

Figure 4: a) Isometric view of Cubesat directional magnetic fluid density, b) Cubesat directional magnetic fluid density, c) Cubesat total force.

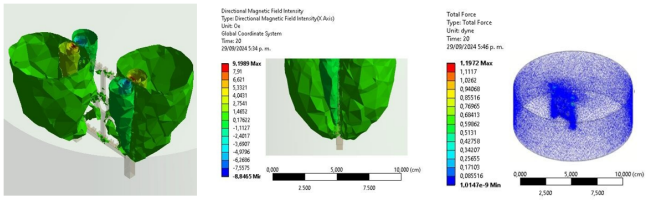

a) b) c)

Source: Own.

Figure 4.a and 4.b represent the directional magnetic fluid

density of the CubeSat which allows us to observe that there is a density of approximately 1.5885 Oe while figure 4.c allows us to analyze the total force that the CubeSat will generate, where it was determined that in most of the structure the force is very small, which will facilitate and prevent the structure from having physical problems or system location problems, as the case may be.

In the second part of the magneto-static analysis, the copper structure will be subjected to a voltage of 5 mv, which will generate the following results:

Figure 5: a) CubeSat current density, b) Cubesat directional magnetic flux density isometric view, c) Cubesat directional magnetic flux density range.

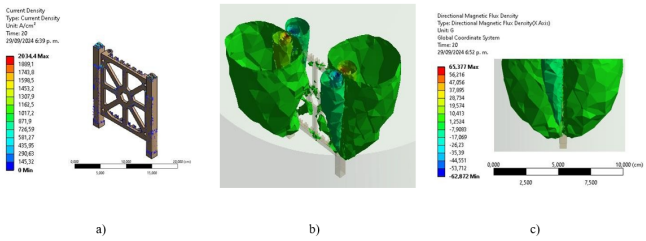

a) b) c)

Source: Own.

Figure 5.a shows the current density simulation, which allows analyzing the current passing through a cross section of the CubeSat structure. It is observed that the applied voltage generates a high current density, which could cause damage due to excessive overheating. The directional magnetic flux density simulations, presented in Figures 5.b and 5.c, reveal a magnetic flux close to 1.252 Gauss, with an approximate range of 5 cm from the structure.

Figure 6: a) Isometric view of Cubesat directional magnetic fluid density, b) Cubesat directional magnetic fluid density, c) Cubesat total force.

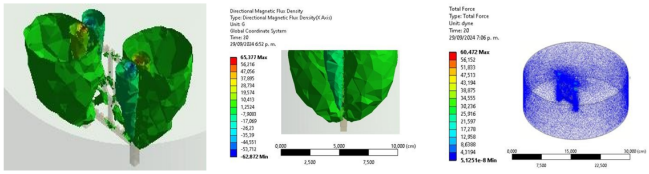

a) b) c)

Source: Own.

Figure 6.a and 6.b represent the density of the directional magnetic fluid of the CubeSat which allows us to observe that there is a density of approximately 1.252 Oe while figure 6.c allows us to analyze the total force that the CubeSat will generate, where it was determined that in most of the structure the force is very small, which will facilitate and prevent the structure from having physical or system location problems, as the case may be.

In the third part of the magneto-static analysis, the structure made of aluminum will be subjected to a voltage of 10 mv, taking into account that it is the most common material of the Cubesat and will generate the following results:

Figure 7: a) CubeSat current density, b) Cubesat directional magnetic flux density isometric view, c) Cubesat directional magnetic flux density range.

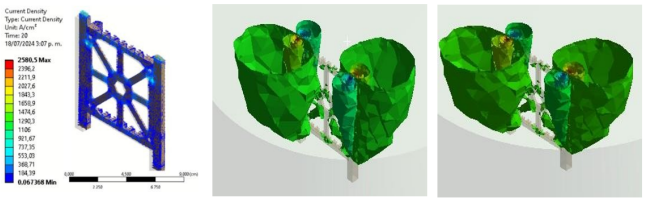

a) b) c)

Source: Own.

Figure 7.a shows the current density simulation, which allows analyzing the current passing through a cross section of the CubeSat structure. It is observed that the applied voltage generates a high current density, which could cause damage due to excessive overheating. The simulations of the directional magnetic flux density, presented in Figures 7.b and 7.c, reveal a magnetic flux close to 1.5885 Gauss, with an approximate range of 10 cm from the structure.

Figure 8: a) Isometric view of Cubesat directional magnetic fluid density, b) Cubesat directional magnetic fluid density, c) Cubesat total force.

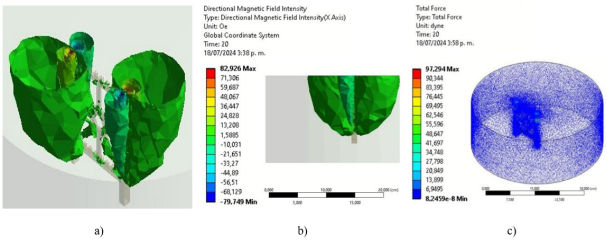

a) b) c)

Source: Own.

Figure 8.a and 8.b represent the directional magnetic fluid density of the CubeSat which allows us to observe that there is a density of approximately 1.5885 Oe while figure 8.c allows us to analyze the total force that the CubeSat will generate, where it was determined that in most of the structure the force is very small, which will facilitate and prevent the structure from having physical problems or system location problems, as the case may be.

Finally after observing and analyzing the respective materials it was determined that the material that has the most efficient behavior is copper because it needs little voltage to generate the respective magnetic fluxes, along with its economic advantage because it is the most economical material among those proposed, but it will have the second highest current which will generate possible deformations of the system taking into account the capabilities of the material.

It should be clarified that the structure will also have other limitations due to the components that are inside which, being conductors, can generate shorts or other electrical or electronic problems.

1.3.3. Mechanical analysis

In Figure 9, it can be observed how the forces and the calculated acceleration for the CubeSat 1U were positioned, which subsequently allows for the simulation of the total and elastic deformation of the structure, as well as the equivalent stress.

Figure 9: Diagram of the forces acting on the CubeSat during the launch stages.

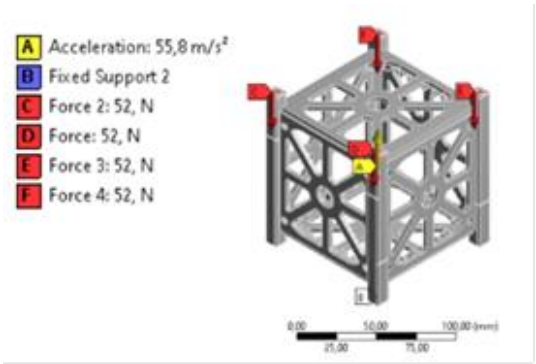

Source: Own.

Subsequently, the analysis of total deformation, equivalent stress, and equivalent elastic deformation in each of the materials is presented.

Figure 10: Diagram of the forces acting on the CubeSat during the launch stages.

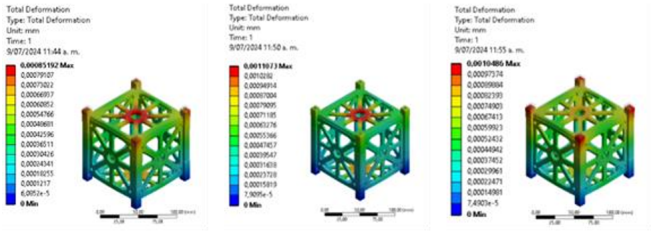

a) b) c)

Source: Own.

First, the total deformation of the structure in each of the materials is evaluated, measured in millimeters. The simulation shown in Figure 10.a presents the results for titanium, with a maximum deformation of 0.00085192 mm. Similarly, Figure 10.b shows the results for copper, with a maximum total deformation of 0.0011073 mm. Finally, in Figure 10.c, the total deformation for aluminum is observed, with a maximum of 0.0010486 mm.

Figure 11: Equivalent elastic deformation in mm/mm of the CubeSat. a) Titanium, b) Copper, c) Aluminum.

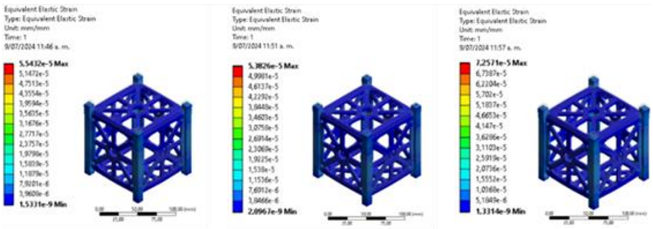

a) b) c)

Source: Own.

Subsequently, the equivalent elastic deformation is evaluated in mm/mm. The simulation shown in Figure 11.a presents the results for titanium, with a maximum of 5.5 × 10-5 mm/mm. Figure 11.b shows the result for copper, with a maximum of 5.3 × 10-5 mm/mm, while Figure 11.c displays the result for aluminum, with a maximum of 7.2 × 10-5 mm/mm.

As observed in the simulations, the areas with the highest equivalent elastic deformation are the tips of the CubeSat, where the loads induced by the launch are applied. However, the deformation does not vary significantly in relation to the faces of the cube.

Figure 12: Von Mises stress in MPa of the CubeSat. a) Titanium, b) Copper, c) Aluminum.

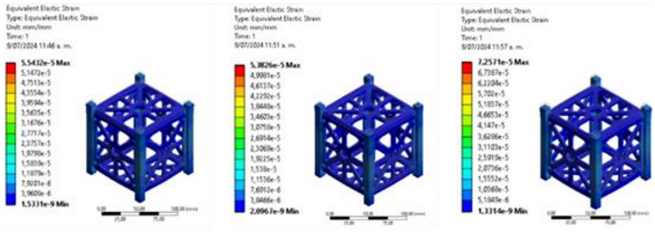

a) b) c)

Source: Own.

Similarly, the von Mises stresses in the structure are analyzed, measured in MPa. The simulation in Figure 12.a presents the result for titanium, with a maximum of 5.3 MPa. Figure 12.b shows the result for copper, with a maximum of 5.9 MPa, while Figure 12.c displays the result for aluminum, with a maximum of 5.1 MPa. For all three materials, the maximum stress is around 5 MPa, which is not a considerable stress when compared to the yield strength of these materials.

2. Conclusions

The simulation results reveal that the higher the emissivity, as in the case of titanium, the more heat the system emits to the surroundings, which reduces the equilibrium temperature. In contrast, materials with low emissivity such as copper and aluminum tend to retain more heat, raising their equilibrium temperatures.

The simulation showed considerable differences in heat flux between the materials, both in the amount of heat absorbed and emitted. Titanium, with the lowest outgoing heat flux rate (122 W/m²), and copper with the highest rate (901.2 W/m²), reflect the variation in heat transfer depending on the material and its properties. This behavior is crucial for the thermal design of CubeSats, where it is necessary to balance heat input and output to avoid thermal failure of sensitive components.

The material that has a better behavior is copper, because with a low voltage it generates the desired magnetic flux but with a high current, on the contrary, titanium would be the material that has more balance in terms of current, because with a high voltage the power needed by the structure to achieve the desired magnetic flux is reduced.

References

[1] R. Seetharaman, A. Singh, R. S. Sumit, J. Krishnaprasad, S. Nazim, and G. Watts, "Modal, Static Structural and Transient Thermal Analysis Of A Standard 1u Cubesat," 2019. doi: 10.13140/RG.2.2.34054.52805.

[2] L. Pablo, I. Olmedo Fernando, and I. Fernandez Edgardo, "Análisis y simulación del comportamiento térmico del sistema integrado, estructura y componentes electrónicos del prototipo del nanosatélite Cubesat," [Technical Report].

[3] R. C. CABRIALES, L. A. REYES, C. CHÁVEZ, D. COBOS, and P. C. ZAMBRANO-ROBLEDO, "ANÁLISIS Y SIMULACIÓN DE TRANSFERENCIA DE CALOR EN ÓRBITA DE UN CUBESAT USANDO iOS," *Revista Ciencia UANL*, vol. 23, no. 103, Sep. 2020. doi: 10.29105/cienciauanl23.103-1.

[4] S. Kubade, S. Kulkarni, and P. Dhatrak, "TRANSIENT THERMAL ANALYSIS OF 1U MODULAR CUBESAT BASED ON PASSIVE THERMAL CONTROL SYSTEM," *Archives of Metallurgy and Materials*, vol. 68, no. 4, pp. 1247–1254, 2023. doi: 10.24425/amm.2023.146189.

[5] R. De la Vega Ibarra, B. Romero Ángeles, D. Torres Franco, A. Molina Ballinas, and L. A. De la Vega Ibarra, "Análisis de resistencia estructural en el diseño de un nanosatélite CubeSat," *Científica*, vol. 23, pp. 141–148, Apr. 2019. [Online]. Available: https://www.redalyc.org/journal/614/61459623007/html/.

[6] Alén Space, "Guía básica de nanosatélites." [Online]. Available: https://alen.space/es/guia-basica-de-nanosatelites/. (Accessed: Jul. 22, 2024).

[7] J. E. Herrera Arroyave, "Diseño estructural de un sistema CubeSat con recubrimiento de barrera térmica," Universidad Autónoma de Nuevo León, San Nicolás de los Garza, 2015.

[8] J. Ling, R. Lamniji, and R. Stewart, "Magnetorquer," *ECE 445*, pp. 1–19, Dec. 07, 2019.

[9] SATNOW, "Magnetorquer for satellite applications." [Online]. Available: https://www.satnow.com/products/magnetorquers/chang-guang-satellite-technology/41-1221magnetorquer-chang-guang-satellite. (Accessed: Jul. 09, 2024).

[10] J. Ling, R. Lamniji, and R. Stewart, "Magnetorquer," *ECE 445*, pp. 1–19, Dec. 07, 2019.

[11] SATNOW, "Magnetorquer for satellite applications." [Online]. Available: https://www.satnow.com/products/magnetorquers/chang-guang-satellite-technology/41-1221magnetorquer-chang-guang-satellite. (Accessed: Jul. 09, 2024).